

Cisplatin alters the function and expression of N-type voltage-gated calcium channels in the absence of morphological damage of sensory neurons

Markus Leo¹, Linda-Isabell Schmitt¹, Holger Jastrow²,
Jürgen Thomale³, Christoph Kleinschnitz¹ and Tim Hagenacker¹

Abstract

Platinum-based chemotherapeutic agents, such as cisplatin, are still frequently used for treating various types of cancer. Besides its high effectiveness, cisplatin has several serious side effects. One of the most common side effects is dorsal root ganglion (DRG) neurotoxicity. However, the mechanisms underlying this neurotoxicity are still unclear and controversially discussed. Cisplatin-mediated modulation of voltage-gated calcium channels (VGCCs) in the DRG neurons has been shown to alter intracellular calcium homeostasis, a process critical for the induction of neurotoxicity. Using the whole-cell patch-clamp technique, immunostaining, behavioural experiments and electron microscopy (EM) of rat DRGs, we here demonstrate that cisplatin-induced neurotoxicity is due to functional alteration of VGCC, but not due to morphological damage. In vitro application of cisplatin (0.5 μ M) increased N-type VGCC currents ($I_{Ca(V)}$) in small DRG neurons. Repetitive in vivo administration of cisplatin (1.5 mg/kg, cumulative 12 mg/kg) increased the protein level of N-type VGCC over 26 days, with the protein level being increased for at least 14 days after the final cisplatin administration. Behavioural studies revealed that N-type VGCCs are crucial for inducing symptoms of cisplatin-related neuropathic pain, such as thermal and mechanical hyperalgesia. EM and histology showed no evidence of any structural damage, apoptosis or necrosis in DRG cells after cisplatin exposure for 26 days. Furthermore, no nuclear DNA damage in sensory neurons was observed. Here, we provide evidence for a mainly functionally driven induction of neuropathic pain by cisplatin.

Keywords

neurotoxicity, voltage-gated calcium channels, neuropathic pain, dorsal root ganglia

Date received: 17 September 2017; revised: 24 October 2017; accepted: 1 November 2017

Introduction

Platinum-based chemotherapeutic agents play a major role in the treatment of various cancers. In addition to its high anti-neoplastic efficacy, treatment with cisplatin leads to several side effects, of which dorsal root ganglion (DRG) neurotoxicity is the most considerable, as it leads to painful peripheral polyneuropathy.^{1,2} Pain in chemotherapy-induced neuropathy (CIPN) is characterized by typical symptoms, such as mechanical allodynia and thermal hyperalgesia.³ While the anti-cancer effects of platinum-compounds are well understood, the neurotoxic mechanisms involved still remain unclear.

The accumulation of unrepaired platinum–DNA crosslinks in the cell nucleus is essential for the toxicity

in cancer cells, but also suggested to be a key mechanism of cisplatin toxicity in sensory neurons.^{1,2,4,5} Interaction of platinum-based chemotherapeutic agents, such as cisplatin or oxaliplatin, with DNA leads to intrastrand and interstrand DNA cross-linkage, resulting in denaturation of nuclear and mitochondrial DNA. This damage causes the death of the cancer cells by activating necrotic and

¹Department of Neurology, University Hospital Essen, Essen, Germany

²Institute of Anatomy, University Hospital Essen, Essen, Germany

³Institute for Cell Biology, University of Duisburg-Essen, Essen, Germany

Corresponding author:

Tim Hagenacker, Department of Neurology, University Hospital Essen, Hufelandstrasse 55, D-45122 Essen, Germany.

Email: tim.hagenacker@uk-essen.de



apoptotic pathways.⁶ Within sensory neurons, cisplatin and oxaliplatin induce nuclear and mitochondrial DNA damage, resulting in mitochondrial dysfunction and the generation of reactive oxygen species.⁷ Besides those DNA damage mechanisms, several studies have shown a disturbance of intracellular calcium homeostasis after platinum-compound treatment. This disturbance is linked to a critical increase in intracellular calcium concentration in various cell types, including sensory neurons within the DRG.^{8,9} Intracellular calcium is a second messenger for initiation of numerous cellular processes, such as transmitter release, regulation of apoptosis or intracellular signalling. Calcium ions can enter neurons by voltage-gated calcium channels (VGCCs). The VGCC protein family consists of various subtypes, namely L-, T- P-/Q- and N-type calcium channels, which differ in their physiological functions, electrophysiological properties and subcellular localization.^{10,11} The functional regulation of VGCC is mediated by intracellular calcium-dependent protein kinases.^{12,13} In addition to the excitatory function of VGCC, the mediated calcium influx is involved in calcium-dependent activation of gene expression processes, that is by activation of calmodulin (CaM) and calcium/calmodulin-dependent kinases (CaMK).

Recent studies revealed VGCC and its currents ($I_{Ca(V)}$) to be involved in the pathogenesis of painful neuropathies after nerve injury.¹⁴ Modulation of function and expression of N-type VGCC seem to be linked with the onset of neuropathic symptoms.^{15–18} Recently, we have provided evidence for an involvement of N-type VGCC in cisplatin-induced peripheral neurotoxicity.¹⁹

In this study, we examined the role of N-type VGCC in a rat model of cisplatin-induced peripheral neuropathy with neuropathic pain using the in vitro whole-cell patch-clamp technique, immunohistochemistry, electron microscopy (EM) and behavioural experiments after in vivo cisplatin treatment.

Materials and methods

Animals

Three- to four-week-old male and female Wistar rats (60–80 g, Animal Research Laboratory, University of Duisburg-Essen, Germany) were used for in vitro electrophysiology. For behavioural experiments, male Sprague-Dawley rats (120–150 g, Charles River, Germany) were used. All experiments were performed in accordance with the guidelines of the animal care and use committees of the University of Duisburg-Essen, Germany, and the ARRIVE guidelines. All rats were kept under a 14/10-h light/dark cycle with water and standard food pellets available ad libitum.

Cell culture of DRG neurons

DRGs were removed from rats and the neurons isolated, as described previously.²⁰ A 50- μ l amount of cell suspension was placed in the centre of each cell culture dish (35 mm, Falcon “Easy Grip”). Neurons were incubated for at least 2 h to allow for cell adhesion. A 1-ml amount of F12 medium containing 10% horse serum (Biochrom AG, Germany) was added to each dish and the neurons were placed in the incubator at 37°C and 5% CO₂ until use in the patch-clamp experiments the next day.

Electrophysiology

Whole-cell recording. $I_{Ca(V)}$ s of N-type VGCC were isolated using the whole-cell patch-clamp technique with a HEKA EPC 10 amplifier and Patchmaster software (HEKA Electronics, Germany). Only small DRG neurons with round morphology were selected for the experiments to prevent space-clamp artefacts. Small DRG neurons were characterized by a diameter <25 μ m and a capacity <38 pf. Neurons were used within the next 24 h after isolation. For short-term in vitro treatment of neurons, we used cisplatin at a concentration of 0.5 μ M.

Microelectrodes consisting of borosilicate glass (Biomedical Instruments, Germany) were pulled with a HEKA Pipette Puller (PIP6, HEKA Electronics, Germany) and were fire polished to a final resistance of 5–7 M Ω . Before starting experiments, cell culture medium was replaced with external solution containing MgCl₂ 1 mM, HEPES (4-(2-hydroxyethyl)-1-piperazineethanesulphonic acid) 10 mM, tetrodotoxin 0.001 mM, glucose 10 mM, BaCl₂ 10 mM and tetraethylammonium chloride 130 mM, pH 7.3. The internal pipette solution contained CsCl 140 mM, MgCl₂ 4 mM, HEPES 10 mM, ethylene glycol-bis(β -aminoethyl ether)-N,N,N',N'-tetraacetic acid 10 mM and Na-ATP 2 mM, pH 7.2. For isolating currents of N-type VGCC, other subtypes were inhibited using a mixture of specific channel blockers. Inhibition of T-type $I_{Ca(V)}$ was reached using pimozide (100 nM). For inhibition of L-type and P-/Q-type $I_{Ca(V)}$, nimodipine (L-type, 2 μ M) and ω -agatoxin (P-/Q-type, 0.2 μ M) were used. Neurons were incubated with blockers for 10 min before starting whole-cell recordings.

A gigaohm seal between the electrode and cell membrane was established. Membrane potential was clamped at –80 mV. $I_{Ca(V)}$ was elicited by depolarizing command pulses to 0 mV (150 ms). To examine the current–voltage (I – V) relationship of $I_{Ca(V)}$, DRG neurons were depolarized in increasing 10-mV steps, starting from –60 mV to +50 mV and I – V curves were frequently recorded before and after application of cisplatin.

Data analysis of electrophysiological recordings. All currents were corrected online using a P/4 protocol. All $I_{Ca(V)}$

values used for the time-course experiment were rundown corrected, assuming a linear rundown. The rundown was calculated from the 10 currents elicited before application of cisplatin (control condition). Only cells with a rundown of <3% were included in the data analysis. Current values were standardized to the mean current before application of cisplatin (= 100%).

In vivo treatment of animals

The influence of cisplatin on the protein level of N-type VGCC during cisplatin chemotherapy was examined by treating rats with NaCl (0.9%, intraperitoneally (i.p.)) or with cisplatin (1.5 mg/kg, i.p.).

To examine the influence of cisplatin and the role of N-type VGCC on the pain-associated behaviour of rats in vivo, the rats were treated with either cisplatin (1.5 mg/kg, i.p.) and NaCl (0.9%, intravenously (i.v.)) or with a combination of cisplatin and ω -conotoxin MVIIA (0.02 mg/kg, i.v.).¹⁹

In both experimental approaches, cisplatin was administered in two cycles of four daily injections with a four-day rest between the cycles. ω -conotoxin MVIIA was administered daily for 12 days for behavioural experiments. Six rats were used for each experimental condition in behavioural experiments.

Rats were controlled daily for weight loss during the treatment. If a weight loss of >10% was observed, food pellets were moisturized. If weight loss was >20%, rats were sacrificed.

Immunohistochemical staining

Tissue preparation. Cisplatin-treated and untreated rats were sacrificed at different time points (3, 6, 11, 16, 23 and 26 days) of the experiment. The DRGs (L4-L6) were removed from three rats for each condition per time point; 8- μ m-thick slices were prepared and placed on microscopic slides.

Tissue sections were fixed in ice-cold methanol for 20 min at -20°C . Cell membranes were permeabilized in phosphate-buffered saline (PBS) + 0.5% Triton X-100 for 15 min at room temperature. Unspecific binding sites were blocked with 5% milk powder in PBS for 1 h at room temperature. To investigate the protein level of N-type VGCC, tissue sections were incubated overnight with rabbit primary antibody against N-type VGCC subtype (1:200, anti-CaV2.2, Alomone Labs, Israel) at 4°C . After washing (PBS), sections were incubated with secondary antibody (goat anti-rabbit Alexa Fluor 555, Thermo Fisher Scientific) for 1 h in darkness at room temperature.

Data analysis of immunohistochemical staining. The N-type VGCC protein levels were quantified using Image J

software (NIH). Neurons were selected using the Free Hand tool. The integrated density of N-type VGCC in DRG neurons with each slice was measured and normalized against the background.

All data were analyzed using analysis of variance (ANOVA) and Turkey's post hoc test compared with control. All data are reported as means \pm SEM ($p < 0.05$ was regarded as statistically significant).

Western blot

For western blot analysis, DRGs (L4-L6) were removed at day 11 and day 26. Untreated DRGs served as control. The tissue was homogenized in radioimmunoprecipitation assay buffer (Thermo Fisher Scientific). Proteins were transferred to nitrocellulose membranes (0.2 μm) using wet blot technique at 4°C for 2 h. Membranes were blocked in Tris-buffered saline supplemented with Tween-20 (TBST) containing 5% nonfat milk powder (Sigma Aldrich) for 1 h at room temperature with gentle agitation. Membranes were incubated overnight at 4°C with rabbit polyclonal N-type alpha 1B (1:200, Alomone Labs) and mouse monoclonal beta-actin (1:1000, Thermo Fisher Scientific) antibodies. Afterwards, membranes were incubated with anti-rabbit IgG and anti-mouse IgG horseradish peroxidase coupled secondary antibodies (1:1000, Thermo Fisher Scientific) for 2 h at room temperature. Immunoreactivity was detected using "Enhanced Chemiluminescence Substrate" (Thermo Fisher Scientific).

Analysis of western blot signals was performed using Image J software (NIH). Intensity of N-type VGCC was normalized to intensity of beta-actin.

Behavioural experiments

Baseline data were recorded daily for 3 h, before treatment of the rats. Drugs were administered from day 4 to day 15. Behavioural experiments were performed on days 8, 17, 24 and 31.

Hot-plate testing and von Frey testing. Thermal hyperalgesia was assessed with an algesimeter (Ugo Basile, Comerio, Italy), as described previously.^{19,21} Three consecutive thermal tests were applied to the rats' hindpaws with at least a 5-min interval between tests for an individual paw. The means of three tests were calculated.

Mechanical sensitivity was assessed using von Frey hairs and the up-down method.²² Thereby the 50% probability withdrawal threshold was determined.

Data analysis of behavioural experiments. All data were analyzed using ANOVA and Tukey's post hoc test

compared with control. All data are reported as means \pm SEM.

Quantification of cisplatin-induced DNA adducts

Visualization of cisplatin-induced DNA adducts was performed as described elsewhere.^{4,23} Frozen sections of DRGs (8 μ M) were prepared from collected tissue of repetitive cisplatin-treated rats after performing behavioural experiments (day 31). Sections were placed onto Superfrost Plus Gold adhesion slides (Thermo Scientific) to prevent cell loss during additional processing.

DRG sections were fixed in ice-cold methanol (-20°C) and rehydrated in PBS. After partial denaturation, tissues sections were subjected to a two-step proteolytic digestion. First, DRGs were treated with pepsin (300 $\mu\text{g}/\text{ml}$) for 10 min at 37°C ; after this, the tissue sections were treated with proteinase K (100 $\mu\text{g}/\text{ml}$, pH 7.5) for 10 min at 37°C . Cisplatin-(GG) adducts in the nuclear DNA of DRG neurons were stained with adduct-specific monoclonal antibody R-C18 and goat-anti rabbit Cy3 (red) secondary antibody.

Haematoxylin–eosin staining

Rats were sacrificed after behavioural experiments on day 31, DRG were resected, fixed in formalin and embedded in paraffin. For haematoxylin–eosin (HE) staining, tissue sections (8 μm) were fixed with acetone for 3 min at -20°C and then placed in methanol (80%) for 5 min at 4°C . After fixation, the tissue sections were washed in PBS for 10 min. DRG sections were stained with haematoxylin for 1 min and washed in aqua bidest for 5 min. Eosin staining was performed for 30 s. Tissue was successively placed in 70%, 80%, 90% and 100% ethanol for 5 min in each concentration. The sections were treated twice with xylene for 5 min and dried completely. Permount was used to mount slides.

Electron microscopy

Tissue samples of about 1 mm³ were fixed overnight in 100 mM phosphate buffer (PB) containing 2.5% glutaraldehyde, 3 \times washed in PB at room temperature and treated with 1% (w/v) OsO₄ for 2.5 h on ice. This was followed by washing in PB for 3 \times 10 min at 4°C and ethanol 30% and 50% (35 min each). Then 1% uranylacetate was applied in 70% ethanol in darkness for block contrast for 1 h. Blocks were then kept in 70% ethanol at 4°C overnight. After 96% ethanol (35 min), pure ethanol then propylene oxide were applied for 3 \times for 10 min each followed by EPON[®] solutions in ethanol with an increasing EPON[®] concentration (3:1, 1:1, 1:3; 60 min each) and finally pure EPON[®] overnight at room

temperature. Embedding was performed in a heated storage area (60°C , 2 days) for polymerization. After trimming, solid EPON[®] blocks were cut on a Reichert-Jung Ultracut[®] ultramicrotome set to a thickness of 70 nm. Sections were then mounted on 200 mesh hexagonal copper grids and treated with 1% uranyl acetate solution for 20 min. This was followed by 5 min of lead citrate (0.4%) for contrast enhancement. A Zeiss transmission electron microscope (EM 902A) was used for the final investigation at 80 kV at magnifications from 3000 \times to 140,000 \times . Digital image acquisition was performed by a MegaViewII slow-scan-CCD camera connected to a personal computer running ITEM[®] 5.0 software (Soft-imaging-systems, Münster, Germany); the images were stored as uncompressed TIFF files in 16 bits of grey and further processed using Adobe[®] Photoshop[®] CS5.

For analyzing structural damage after repetitive cisplatin treatment, we have randomly chosen five images per condition and counted profiles of damaged mitochondria.

Results

Cisplatin increases currents of N-type VGCC

N-type $I_{\text{Ca}(\text{V})}$ was isolated using combinations of specific VGCC subtype blockers, as described earlier. To examine the influence of cisplatin on N-type $I_{\text{Ca}(\text{V})}$, the whole-cell patch-clamp technique was used. Depolarization of DRG neurons from holding potential (-80 mV) to 0 mV elicited an inward current through N-type VGCC. Cisplatin (0.5 μM) led to an increase in N-type $I_{\text{Ca}(\text{V})}$ (Figure 1(a)) of $131.1 \pm 5.2\%$. Steady-state was reached after 300 s (Figure 1(b)). In I - V experiments, the peak current was elicited at a depolarization of up to -30 mV under control conditions. Cisplatin increases the $I_{\text{Ca}(\text{V})}$ in a voltage range of -60 mV to $+50$ mV. A shift of the peak current or changes of the reversal potential were not observed (Figure 1(c)).

Repetitive in vivo administration of cisplatin increases N-type VGCC protein level transiently

To examine the influence of cisplatin on the protein level of N-type VGCC in vivo, rats were repetitively treated. Treatment was performed as described earlier. Cisplatin was administered in two, four-day cycles (Figure 2(a)). Rats were sacrificed on days 3, 6, 11, 16, 23 and 26. DRG tissue sections were prepared and immunohistochemical staining against N-type VGCC was performed (Figure 2(b)).

Repetitive in vivo administration of cisplatin increased the N-type protein level significantly over the entire experimental time, compared with untreated

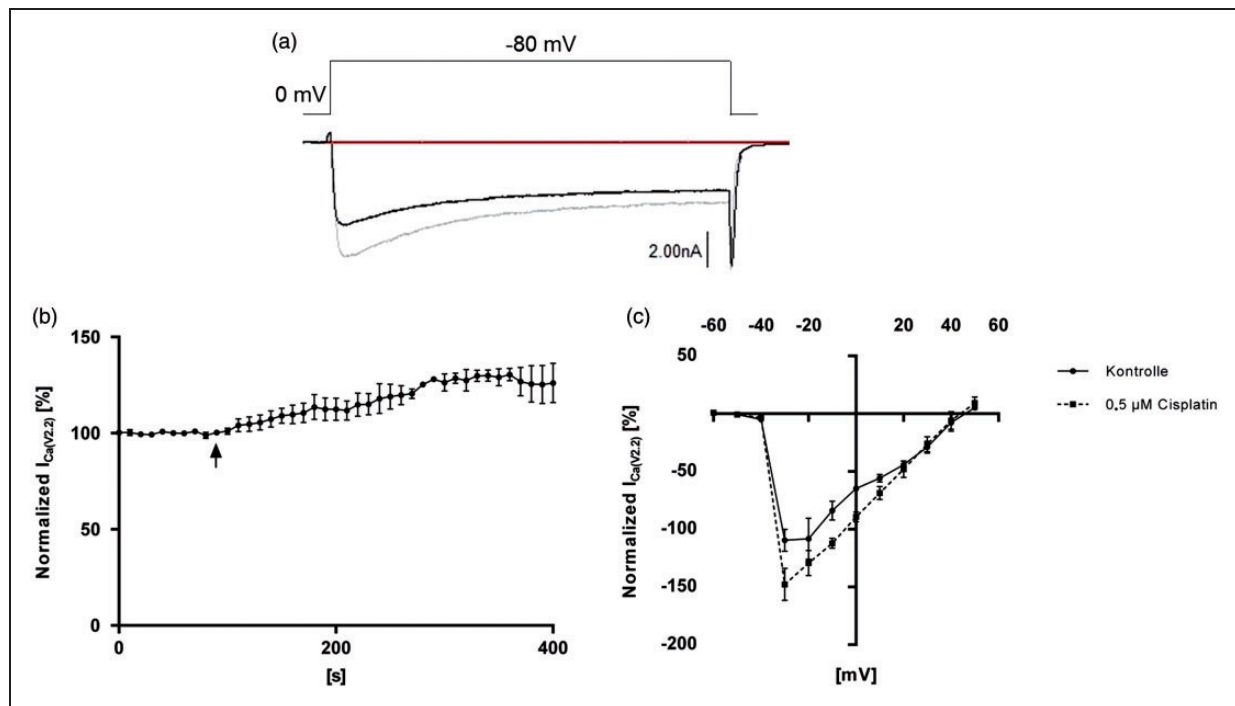


Figure 1. Modulation of N-type $I_{Ca(V)}$ by cisplatin in small dorsal root ganglion (DRG) neurons in vitro. (a) Representative raw trace of N-type $I_{Ca(V)}$. DRG neurons were depolarized from the holding potential (-80 mV) to 0 mV before (black line) and after (grey line) application of cisplatin (0.5 μ M). Application of cisplatin led to an increase in N-type $I_{Ca(V)}$. (b) Time-course measurement of normalized $I_{Ca(V)}$ of isolated N-type voltage-gated calcium channels (VGCCs) during repetitive depolarizations from the holding potential to 0 mV before and after application of 0.5 μ M cisplatin. Cisplatin application led to an increase in N-type $I_{Ca(V)}$ over the time. Black arrow marks time of cisplatin application. (c) I - V curve of N-type $I_{Ca(V)}$ (black line, control conditions; speckled line, after application of 0.5 μ M cisplatin). DRG neurons were stepwise (10 -mV increments) depolarized from holding potential to $+50$ mV. Cisplatin application led to an increase in N-type $I_{Ca(V)}$ over the entire voltage range. ($n = 5$ cells for each experiment).

controls. On day 3, the N-type protein level of cisplatin-treated rats had increased to 2.70 ± 0.04 ($*p < 0.05$), compared with untreated rats (1 ± 0.10). When the N-type protein level was determined on day 11, it had significantly increased to 3.54 ± 0.18 ($*p < 0.05$; $\#p < 0.05$), compared with day 6 (2.40 ± 0.07) and with untreated control (1 ± 0.10). The protein level stayed constant until day 16 (3.37 ± 0.09) ($*p < 0.05$). On day 23, the N-type protein level had significantly decreased (2.41 ± 0.13), compared with day 16 ($\#p < 0.05$), but had still increased in comparison with control rats ($*p < 0.05$). Also 14 days after the last cisplatin administration (day 26), the N-type protein level had significantly increased (2.36 ± 0.19), compared with control ($*p < 0.05$). For substantiating those results, we performed western blot analysis on day 11 and day 26. Also here, N-type VGCC protein level was significantly increased on day 11 (2.93 ± 0.1) ($*p < 0.05$) and day 26 (1.94 ± 0.18) ($*p < 0.05$), compared with untreated control DRG tissue (1 ± 0.01). N-type VGCC protein level on day 26 was decreased, compared with day 11 ($\#p < 0.05$) (Figure 2(c)).

Cisplatin-mediated pain-associated behaviour is abolished by inhibiting N-type VGCC

To examine the role of N-type VGCC in neuropathic pain after cisplatin-treatment, rats were repetitively treated with cisplatin (1.5 mg/kg) or a combination of cisplatin (1.5 mg/kg) and specific N-type channel blocker ω -conotoxin MVIIA (0.2 mg/kg), and pain-associated behaviour was tested as described earlier (Figure 3(a)). Fifty percent of the cisplatin-treated rats showed a weight loss of $>10\%$ for the duration of the administration phase. No rats showed a weight loss of $>20\%$. Administration of ω -conotoxin MVIIA was well tolerated by the rats without observing side effects.

In hot-plate testing to examine signs of thermal hyperalgesia, the paw-withdrawal threshold was 16.29 ± 0.98 s under control conditions (days 1–3). After treatment with cisplatin + NaCl, it significantly decreased over the entire experimental time ($*p < 0.05$). After 31 days, threshold had decreased to 9.98 ± 0.19 s. In contrast, rats additionally treated with ω -conotoxin MVIIA showed a significant increase in the paw-withdrawal

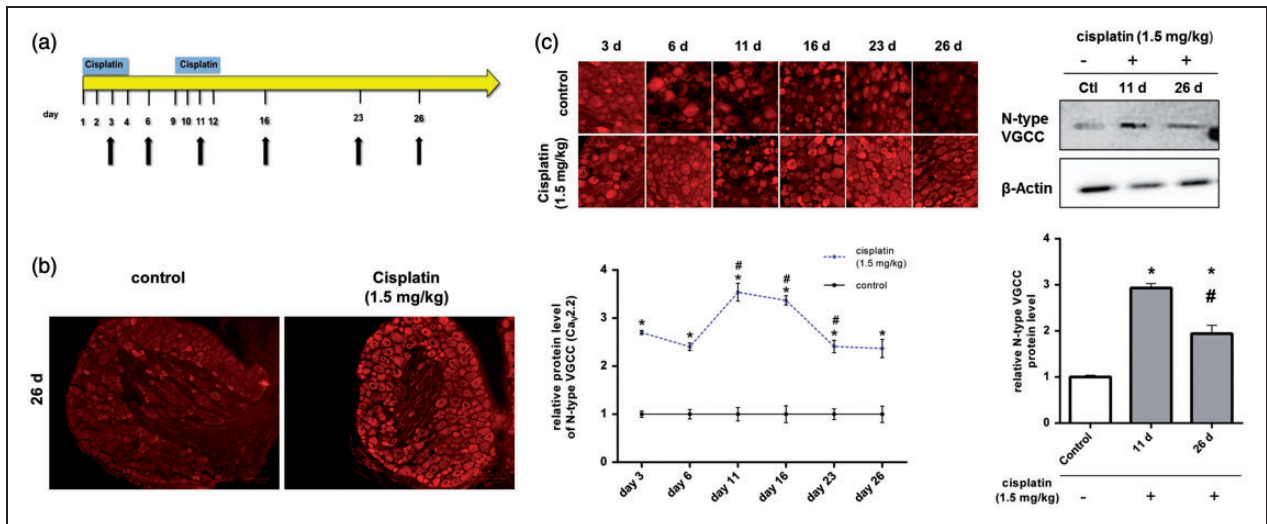


Figure 2. Alteration of the N-type voltage-gated calcium channels (VGCCs) protein level in dorsal root ganglion (DRG) neurons after repetitive *in vivo* administration of cisplatin. (a) To examine the influence of repetitive *in vivo* administration of cisplatin on the protein level of N-type VGCC in DRG neurons, rats were treated with cisplatin (1.5 mg/kg, *i.p.*). Cisplatin was administered in two, four-day cycles, with a four-day break between those cycles. Rats were sacrificed at different time points (black arrows) and immunohistochemical staining against N-type VGCC was performed. Untreated rats served as control. (b) Representative staining of DRGs against N-type VGCC protein (red) 14 days after the last cisplatin administration (day 26). (c) Immunohistochemical staining of DRGs against N-type VGCC protein (red) at different time points (see Figure 2(a), black arrows). Quantification of N-type VGCC-derived signals revealed a significant increase in the protein levels in DRG neurons after cisplatin administration at all tested time points, compared with untreated control DRGs ($*p < 0.05$). Additionally, each day was compared with the day before ($\#p < 0.05$). Here, the protein level of N-type VGCC decreased from day 11 to day 26, but had still increased compared with the control. In western blot analysis, cisplatin administration led to an increase of N-type VGCC protein level on day 11 and day 26 ($*p < 0.05$). Protein level was significantly decreased on day 26, compared to day 11 ($\#p < 0.05$) ($n = 18$ rats in total for each condition).

threshold compared with untreated and cisplatin-treated rats ($\#p < 0.05$). Here, the paw-withdrawal threshold significantly increased to 25.38 ± 0.74 s (Figure 3(b)).

To examine the signs of mechanical allodynia, the von Frey test was used. Untreated rats showed a paw-withdrawal threshold of 21.65 ± 0.1 g. Repetitive administration of cisplatin + NaCl led to a decrease in withdrawal threshold over the entire experimental time, compared with untreated baseline values ($*p < 0.05$). On the last day of the experiment (day 31), 14 days after the last cisplatin administration, the threshold had decreased to 4.85 ± 0.60 g. This effect could be abolished by additional administration of ω -conotoxin MVIIA. Here, the paw-withdrawal threshold was not significantly altered compared with baseline values, but the threshold was significantly increased in comparison with rats treated with cisplatin + NaCl ($\#p < 0.05$) (Figure 3(c)).

Repetitive *in vivo* cisplatin administration does not lead to DNA damage in DRG neurons

To examine the influence of repetitive cisplatin administration on the *in vivo* formation and/or persistence of DNA damage in DRG neurons, we used an immunocytological assay to visualize specific Pt-adducts in the

nuclear DNA of individual cells. For that, DRG of cisplatin-treated rats were resected on day 31 after the behavioural experiments. In immunostained tissue sections, DRG neurons and surrounding non-neuronal cells, that is predominantly satellite glial cells (SGCs) could be distinguished by the size of their DAPI (4',6-diamidino-2-phenylindole)-stained nuclei. As compared with SGC, neurons regularly displayed much larger nuclei with lower DAPI signals (Figure 4). Furthermore, nuclei of sensory neurons were surrounded by a large number of SGC nuclei. While nuclear DNA of SGC displayed strong Pt-DNA antibody immunoreactivity (red), DNA of sensory neurons was not affected 14 days after the last administration of cisplatin (Figure 4).

Repetitive *in vivo* cisplatin administration does not lead to morphological changes or apoptosis in DRG neurons

After repetitive *in vivo* treatment, rats were sacrificed on day 26, tissue sections of DRG were prepared and HE stained. Furthermore, small tissue blocks were prepared for EM.

Neither morphological changes nor structural damage were observed in DRG neurons either in the HE-stained

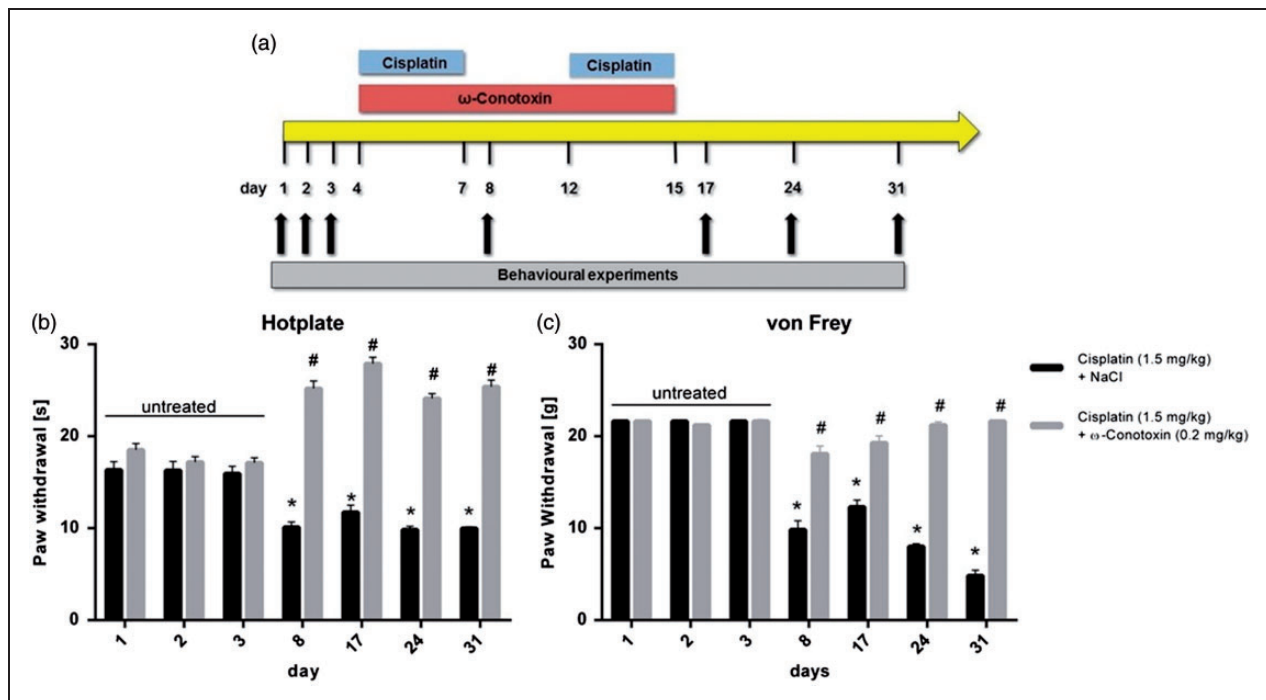


Figure 3. Role of N-type voltage-gated calcium channels (VGCCs) in early signs of cisplatin-induced neuropathic pain. (a) To examine the influence of cisplatin on pain-associated behaviour and the role of N-type VGCC, rats were repetitively treated with either cisplatin (1.5 mg/kg; i.p.) + NaCl (i.v.) or with a combination of cisplatin (1.5 mg/kg; i.p.) + ω-conotoxin MVIIA (0.2 mg/kg; i.v.). The baseline behaviour of untreated rats was recorded on days 1–3. Cisplatin and cisplatin/ω-conotoxin MVIIA administration was started on day 4 until day 15. (b) Rats treated with cisplatin + NaCl showed a significant reduction in the paw-withdrawal threshold in thermal hyperalgesia tests ($*p < 0.05$). When rats were additionally treated with ω-conotoxin MVIIA, a reduction in the paw-withdrawal threshold was not observed, compared with control data. Here the paw-withdrawal threshold was significantly increased ($^{\#}p < 0.05$). (c) Testing mechanical allodynia with von Frey filaments resulted in a significant reduction in the paw-withdrawal threshold of cisplatin + NaCl treated rats, compared with control data ($*p < 0.05$) and to rats treated with cisplatin + ω-conotoxin MVIIA ($^{\#}p < 0.05$). There was no significant change in the paw-withdrawal threshold of rats additionally treated with ω-conotoxin MVIIA, compared with control data ($n = 7$ rats for each condition).

or in ultrathin EM sections when compared with untreated control tissue. Furthermore, we could not detect any indications of apoptosis or necrosis in these neurons after cisplatin administration. Even after long-term cisplatin exposure, no damage of organelles, such as endoplasmic reticulum (ER) or mitochondria, was obvious. Analysis of mitochondria profiles showed no significant difference between control (20.64 ± 3.35 %) and cisplatin-treated (23.55 ± 6.12) DRG neurons on day 26 of the experiment ($p > 0.05$) (Figures 5 and 6).

Discussion

Here, we demonstrate the effects of cisplatin on function and expression of N-type VGCC in DRG neurons and the morphology of DRGs. Our data suggest that alterations in the function and expression of N-type VGCC are the main mediators of neuropathic pain induction after cisplatin treatment.

In several studies, the influence of cisplatin on the calcium homeostasis of various cell types has been described.^{8,24,25} In a recent study, we examined the

effects of cisplatin on VGCC subtypes of DRG neurons in vitro and in vivo.¹⁹ N-type VGCCs are playing a crucial role in pain processing, especially in transmission of pain signals between sensory neurons of the DRG and dorsal horn neurons of the spinal cord.^{15,18,26,27} N-type VGCC knockout mice reveal reduced nociceptive response to sensory stimuli.^{15,18,28}

The N-type protein level rapidly increased after three injections of cisplatin and reached a maximum on day 11 and maintained an increase, to a lower degree, at the end of the experiment. VGCCs are the most common mediators of calcium influx in neuronal cells. An overexpression of these channels may provide a critical increase in intracellular calcium, resulting in toxic calcium-mediated functional and morphological alterations.

Our findings suggest a dependency of the N-type protein level expression, possibly by increased protein translation and/or decreased degradation processes. In several inflammation and nerve lesion models, similar protein-regulation processes have been described. The pro-inflammatory cytokine interleukin 6 increases T-type VGCC in prostate cancer cells.²⁹ After intraplantar

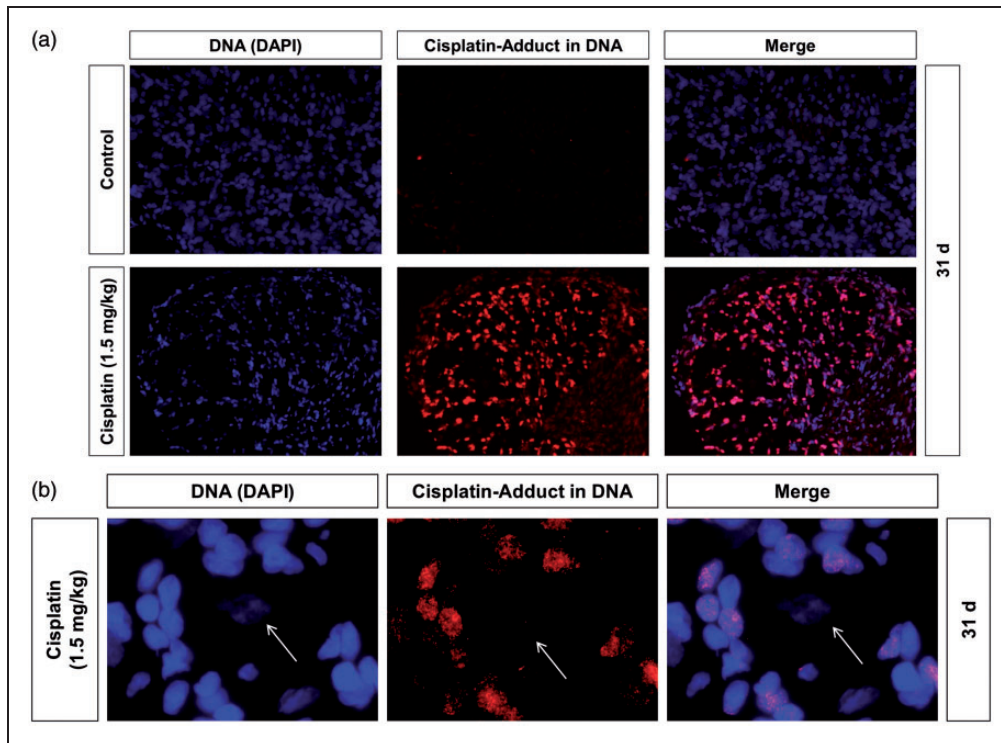


Figure 4. Influence of repetitive in vivo administration of cisplatin on nuclear DNA damage in dorsal root ganglion (DRG) neurons. (a) To examine the levels of nuclear DNA damage in DRG cells of rats after repetitive administration of cisplatin animals were sacrificed on day 31 and DRG cryo-sections were immunostained for Pt-GpG adducts (red) and for DNA (DAPI, blue). DRG tissue of untreated rats served as control. (b) DRG neurons (white arrow) can be distinguished from non-neuronal cells by the size of nuclei. Only a fraction of the non-neuronal cells were positive for cisplatin-induced adducts while DRG neurons were negative ($n = 5$ DRG sections from randomly chosen rats for each condition).

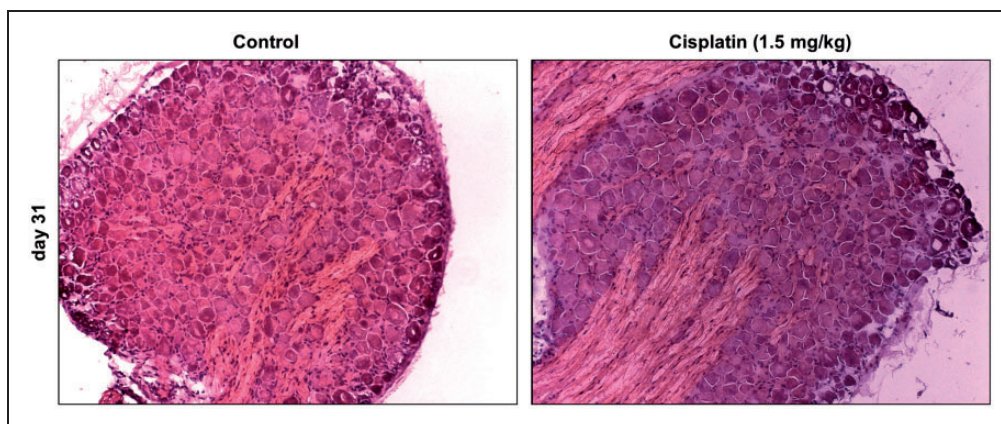


Figure 5. Influence of repetitive in vivo administration of cisplatin on the morphology of dorsal root ganglion (DRG) neurons. In haematoxylin–eosin staining, no morphological changes, structural damage, necrosis or apoptosis could be observed in DRG neurons 14 days after the last in vivo administration of cisplatin (day 26), compared with untreated control DRGs ($n = 3$ DRG slices from randomly chosen rats for each condition).

injection of complete Freund's adjuvant, N-type VGCC protein expression, but not mRNA, is increased in DRG neurons,³⁰ suggesting the involvement of enhanced protein translation processes, rather than gene expression

processes. The upregulation of the $\alpha_2\delta$ -1 subunit of VGCC following peripheral nerve damage has been demonstrated in several animal models of neuropathic pain.^{31–35} The mechanisms leading to the alteration of

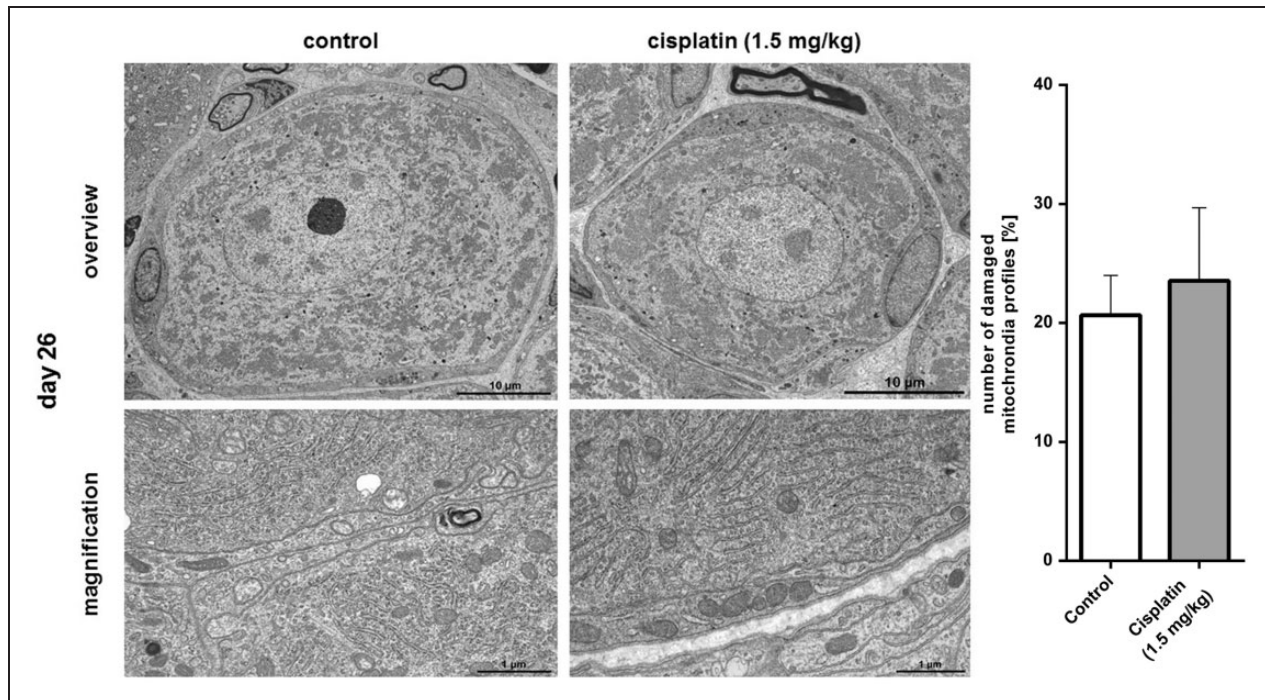


Figure 6. Electron microscopy (EM) of dorsal root ganglion (DRGs) after repetitive in vivo administration of cisplatin. In EM, no morphological changes, structural damage, necrosis or apoptosis could be observed in DRG neurons 14 days after the last in vivo administration of cisplatin (day 26), compared with untreated control DRGs. There was no significant difference between control DRG neurons and neurons after repetitive in vivo cisplatin administration in the number of damaged mitochondria profiles ($*p > 0.05$) ($n = 3$ DRGs from randomly chosen rats for each condition for descriptive study; $n = 5$ randomly chosen images of each condition with at least a total of 750 mitochondria profiles counted).

gene and protein expression after sensory nerve damage are thought to involve propagation of an axonal injury-induced calcium wave to the soma of the sensory neurons, resulting in histone deacetylase 5 export from the nucleus and activation of gene transcription.³⁶ For cisplatin-induced neuropathic pain symptoms, an increase in $I_{Ca(V)S}$ in cultured DRG neurons shortly after cisplatin application was shown to be mediated by protein kinase C activation, while overexpression of N-type calcium channels was shown to be mediated by Ca-calmodulin-kinase II (CaMKII) activation. Here, inhibition of CaMKII by KN-93 resulted in a lack of N-type VGCC overexpression.¹⁹ These results suggest different regulatory mechanisms after cisplatin administration. On the one hand, a short-term mechanism based on ion-channel phosphorylation by protein kinase C.¹⁹ On the other hand, a long-term mechanism regulating the overexpression of the N-type VGCC by CaMKII and further proteins as transcription factors, as similarly shown for the generation of long-term memory in the hippocampus.^{19,37}

Cisplatin treatment reduces the paw-withdrawal thresholds in mechanical and thermal testing during repetitive in vivo administration. The importance of N-type VGCC for the genesis of neuropathic or

inflammatory pain has been shown in studies in knockout mice.^{15,18,28} Pharmacological inhibition of N-type VGCC was able to prevent the signs of neuropathic pain. ω -conotoxin MVIIA was able to reduce mechanical allodynia³⁸ during both the acute and chronic painful stages in an animal model of paclitaxel-induced neuropathy. Recently, we demonstrated the neuroprotective effects of ω -conotoxin MVIIA in cisplatin-induced painful polyneuropathy, outlasting the biological half-life time of 2.9–6.5 h for at least 14 days after the last injection. This protective was mediated by the inhibition of cisplatin-mediated overexpression of N-type VGCC, suggesting N-type VGCC blockade by ω -conotoxin MVIIA to be neuroprotective, besides the well-described analgesia, during chronic pain treatment.¹⁹ The administration of ω -conotoxin MVIIA after increase of N-type VGCC expression would possibly need a higher dose to reach saturation, which possibly will rise the risk of side effects.

Several studies suggested the cisplatin-induced neuropathic pain to be a result of structural damage and loss of function in DRG neurons mediated by cisplatin–DNA adducts following DNA damage.^{1,2,4,5} In clinical studies, the latency period and the severity of signs of neuropathic pain during cisplatin treatment were

cumulative, dose-dependent³⁹ and often outlasting the duration of therapy for several months, the so-called 'coasting effect'. The dose-dependency has often been linked to the platination level of nuclear DNA of DRG neurons.⁴ We demonstrate that no signs of nuclear or morphological neuronal damage could be observed in the early phase after cisplatin treatment, although rats showed clear signs of CIPN. In several studies, it was shown that platination of DNA by cisplatin or oxaliplatin leads to stopping of DNA replication in tumour cells and also to inhibition of ribonucleic acid (RNA) synthesis or protein translation by a blockage of RNA polymerase II.^{40–42} However, due to the post-mitotic nature of neurons and to the results of several studies regarding neurotoxicity of platinum-based chemotherapeutics, it is likely that CIPN is not majorly triggered by platination of nuclear DNA of sensory neurons. Erythropoietin was shown to diminish electrophysiological characteristics of CIPN in mice, without reducing the DNA adduct level in DRG neurons.⁴³ Carboplatin, another platinum-based cytostatic drug, also causes formation of nuclear DNA adducts but only induces a slight CIPN, while oxaliplatin-mediated CIPN is typically very disabling.^{44,45} On the other hand, in the DRG SGC, high DNA platination levels were detectable, while in neurons, no DNA damage was observed, suggesting that DNA platination in the SGC could be involved in the genesis of CIPN, possibly by interfering with neuronal integrity (i.e. local homeostasis, cytokine expression, etc.). Sensory neurons within the DRG do not form synaptic contact between each other, but instead, each soma is tightly enwrapped by a layer of SGC and enclosed by a connective tissue sheath, suggesting an interaction between the neuron, and the SGC is crucial for a correct function and activity of the sensory neurons.^{46–48} If this functional and structural unit is disturbed or even damaged by injury or chemical substances, it is likely that this can affect the sensitivity and ectopic discharges of the neuronal somata, resulting in an alteration in the signalling of the sensory neurons.⁴⁸ The possible role of DNA platination damage in SGC is underscored by the long-term unrepaired persistence of such adducts even two weeks after the last cisplatin administration.

Electron microscopic examination of DRG slices revealed no morphological and structural alterations or apoptosis of DRG neurons after cisplatin treatment. In contrast, it was formerly shown that administration of cisplatin in two cycles of five days led to mitochondrial damage and apoptosis in DRG neurons in mice.⁵ This difference may be explained by the administered cumulative doses of both approaches. While Podratz and colleagues⁵ used a cumulative dose of 23 mg/kg, we used a cumulative dose of 12 mg/kg (1.5 mg/kg per injection).

With a dose of 1.5 mg/kg cisplatin per injection, our low-dose model of cisplatin is in accordance with the literature.⁴⁹ Here, we were able to induce typical signs that polyneuropathy patients commonly suffer, such as thermal and mechanical hyperalgesia, without inducing neuronal death in this early phase of the disease. Beside modulations of VGCC by cisplatin, the modulation of transient receptor potential (TRP) channels as TRPV1 could be an additional option for the induction of thermal hyperalgesia-TRPV1-null, mice developed mechanical allodynia but did not show head-evoked pain responses after cisplatin treatment.⁵⁰ Nevertheless, in the later phase of neuropathy, it could be possible that other mechanisms, such as axonal degeneration or neuronal death, become more important, possibly influenced by a former disturbance of neuronal calcium homeostasis. In a former study, we observed an increased number of activated-caspase-3 positive DRG neurons after in vitro exposure with cisplatin for 24 h. Besides its pro-apoptotic effect, recent studies have also pointed out a nonapoptotic function of this protease in different physiological processes as in the sperm differentiation in the fruitfly *Drosophila*.⁵¹ In 2012, Simon et al.⁵² describe the role of a caspase cascade for the regulation of axonal degeneration. Here, they could show that genetic deletion of caspase-3 is fully protective against sensory axon degeneration that was induced by trophic factor withdrawal, leading to the suggesting of a caspase-3-mediated axonal degeneration in the later phase of cisplatin-induced polyneuropathy.

For the generation of cisplatin-DNA adducts, the transport into the cell is a key mechanism. DRG and tumour cells have a differential expression of transporter proteins for the uptake of cisplatin by copper transporter I (CTR1), and organic cation transporters I and II. In a recent study, the differential expression of copper transporters, such as ATP7A and CTR1, in adult rat DRG tissues was examined. CTR1, which is responsible for the uptake of cisplatin in tissues such as liver or kidney, was strongly expressed in large diameter DRG neurons. In contrast, small neurons did not show a strong expression of CTR1, but for ATP7A, a transporter responsible for the transport of cisplatin out of the cell.⁵³ Axons of small DRG neurons are characterized as c-fibres which are strongly involved in pain processing. The weak expression of CTR1 in small DRG neurons, together with the lack of DNA adducts after cisplatin treatment in our experiments, suggests that generation of cisplatin-DNA adducts in the nucleus is not a relevant mechanism of neurotoxicity.

In this study, we give evidence that cisplatin-induced early phase of neuropathic pain is mainly mediated by alteration in function and expression of ion channels as N-type VGCCs, rather than by morphological changes or structural damage.

Author contributions

Markus Leo: Conceptualization, formal analysis, investigation, visualization and writing – original draft; Linda-Isabell Schmitt: Investigation, formal analysis and writing – original draft; Holger Jastrow: Investigation and writing – review and editing; Jürgen Thomale: Writing – review and editing; Christoph Kleinschnitz: Supervision and writing – review and editing; Tim Hagenacker: Conceptualization, project administration, supervision and writing – review and editing.

Declaration of Conflicting Interests

The author(s) declared no potential conflicts of interest with respect to the research, authorship, and/or publication of this article.

Funding

The author(s) disclosed receipt of the following financial support for the research, authorship, and/or publication of this article: This work was funded by the Deutsche Forschungsgemeinschaft (DFG) (HA6202/4-1) and the Corona-Foundation (S199/10061/2016).

References

1. Thompson SW, Davis LE, Kornfeld M, et al. Cisplatin neuropathy. Clinical, electrophysiologic, morphologic, and toxicologic studies. *Cancer* 1984; 54: 1269–1275.
2. Windebank AJ and Grisold W. Chemotherapy-induced neuropathy. *JPNS* 2008; 13: 27–46.
3. Nickel FT, DeCol R, Jud S, Fasching PA, et al. Inhibition of hyperalgesia by conditioning electrical stimulation in a human pain model. *Pain* 2011; 152: 1298–1303.
4. Dzagnidze A, Katsarava Z, Makhlova J, et al. Repair capacity for platinum-DNA adducts determines the severity of cisplatin-induced peripheral neuropathy. *J Neurosci* 2007; 27: 9451–9457.
5. Podratz JL, Knight AM, Ta LE, et al. Cisplatin induced mitochondrial DNA damage in dorsal root ganglion neurons. *Neurobiol Dis* 2011; 41: 661–668.
6. Eastman A and Barry MA. Interaction of trans-diamminedichloroplatinum(II) with DNA: Formation of monofunctional adducts and their reaction with glutathione. *Biochemistry* 1987; 26: 3303–3307.
7. Jiang Y, Guo C, Vasko MR, et al. Implications of apurinic/aprimidinic endonuclease in reactive oxygen signaling response after cisplatin treatment of dorsal root ganglion neurons. *Cancer Res* 2008; 68: 6425–6434.
8. Spletstoesser F, Florea AM and Busselberg D. IP(3) receptor antagonist, 2-APB, attenuates cisplatin induced Ca²⁺-influx in HeLa-S3 cells and prevents activation of calpain and induction of apoptosis. *Br J Pharmacol* 2007; 151: 1176–1186.
9. Xing C, Chen J and Xu H. [Changes in [Ca²⁺]_i and IP₃ levels in the process of cisplatin-induced apoptosis of gastric carcinoma]. *Zhonghua zhong liu za zhi [Chin J Oncol]* 1999; 21: 256–258.
10. Ertel EA, Campbell KP, Harpold MM, et al. Nomenclature of voltage-gated calcium channels. *Neuron* 2000; 25: 533–535.
11. Lacinova L. Voltage-dependent calcium channels. *Gen Physiol Biophys* 2005; 24(Suppl 1): 1–78.
12. Barrett CF and Rittenhouse AR. Modulation of N-type calcium channel activity by G-proteins and protein kinase C. *J Gen Physiol* 2000; 115: 277–286.
13. Baumgarten LB, Toscas K and Villereal ML. Dihydropyridine-sensitive L-type Ca²⁺ channels in human foreskin fibroblast cells. Characterization of activation with the growth factor Lys-bradykinin. *J Biol Chem* 1992; 267: 10524–10530.
14. Fernyhough P and Calcutt NA. Abnormal calcium homeostasis in peripheral neuropathies. *Cell Calcium* 2010; 47: 130–139.
15. Snutch TP. Targeting chronic and neuropathic pain: the N-type calcium channel comes of age. *NeuroRx* 2005; 2: 662–670.
16. Vanegas H and Schaible H. Effects of antagonists to high-threshold calcium channels upon spinal mechanisms of pain, hyperalgesia and allodynia. *Pain* 2000; 85: 9–18.
17. Vink S and Alewood PF. Targeting voltage-gated calcium channels: developments in peptide and small-molecule inhibitors for the treatment of neuropathic pain. *Br J Pharmacol* 2012; 167: 970–989.
18. Zamponi GW, Lewis RJ, Todorovic SM, et al. Role of voltage-gated calcium channels in ascending pain pathways. *Brain Res Rev* 2009; 60: 84–89.
19. Leo M, Schmitt LI, Erkel M, et al. Cisplatin-induced neuropathic pain is mediated by upregulation of N-type voltage-gated calcium channels in dorsal root ganglion neurons. *Exp Neurol* 2017; 288: 62–74.
20. Hagenacker T, Spletstoesser F, Greffrath W, et al. Capsaicin differentially modulates voltage-activated calcium channel currents in dorsal root ganglion neurons of rats. *Brain Res* 2005; 1062: 74–85.
21. George A, Marziniak M, Schafers M, et al. Thalidomide treatment in chronic constrictive neuropathy decreases endoneurial tumor necrosis factor-alpha, increases interleukin-10 and has long-term effects on spinal cord dorsal horn met-enkephalin. *Pain* 2000; 88: 267–275.
22. Chaplan SR, Bach FW, Pogrel JW, et al. Quantitative assessment of tactile allodynia in the rat paw. *J Neurosci Methods* 1994; 53: 55–63.
23. Liedert B, Plum D, Schellens J, et al. Adduct-specific monoclonal antibodies for the measurement of cisplatin-induced DNA lesions in individual cell nuclei. *Nucleic Acids Res* 2006; 34: e47.
24. Liang X and Huang Y. Intracellular free calcium concentration and cisplatin resistance in human lung adenocarcinoma A549 cells. *Biosci Rep* 2000; 20: 129–138.
25. Tomaszewski A and Busselberg D. Cisplatin modulates voltage-gated channel currents of dorsal root ganglion neurons of rats. *Neurotoxicology* 2007; 28: 49–58.
26. Westenbroek RE, Sakurai T, Elliott EM, et al. Immunochemical identification and subcellular distribution of the alpha 1A subunits of brain calcium channels. *J Neurosci* 1995; 15: 6403–6418.

27. Park J and Luo ZD. Calcium channel functions in pain processing. *Channels* 2010; 4: 510–517.
28. Hatakeyama S, Wakamori M, Ino M, et al. Differential nociceptive responses in mice lacking the alpha(1B) subunit of N-type Ca(2+) channels. *Neuroreport* 2001; 12: 2423–2427.
29. Weaver EM, Zamora FJ, Hearne JL, et al. Posttranscriptional regulation of T-type Ca(2+) channel expression by interleukin-6 in prostate cancer cells. *Cytokine* 2015; 76: 309–320.
30. Lu SG, Zhang XL, Luo ZD, et al. Persistent inflammation alters the density and distribution of voltage-activated calcium channels in subpopulations of rat cutaneous DRG neurons. *Pain* 2010; 151: 633–643.
31. Bauer CS, Nieto-Rostro M, Rahman W, et al. The increased trafficking of the calcium channel subunit alpha2delta-1 to presynaptic terminals in neuropathic pain is inhibited by the alpha2delta ligand pregabalin. *J Neurosci* 2009; 29: 4076–4088.
32. Luo ZD, Chaplan SR, Higuera ES, et al. Upregulation of dorsal root ganglion (alpha)2(delta) calcium channel subunit and its correlation with allodynia in spinal nerve-injured rats. *J Neurosci* 2001; 21: 1868–1875.
33. Newton RA, Bingham S, Case PC, et al. Dorsal root ganglion neurons show increased expression of the calcium channel alpha2delta-1 subunit following partial sciatic nerve injury. *Brain Res Mol Brain Res* 2001; 95: 1–8.
34. Matsumoto M, Inoue M, Hald A, et al. Inhibition of paclitaxel-induced A-fiber hypersensitization by gabapentin. *J Pharmacol Exp Ther* 2006; 318: 735–740.
35. Nieto-Rostro M, Sandhu G, Bauer CS, et al. Altered expression of the voltage-gated calcium channel subunit alpha(2)delta-1: a comparison between two experimental models of epilepsy and a sensory nerve ligation model of neuropathic pain. *Neuroscience* 2014; 283: 124–137.
36. Cho Y, Sloutsky R, Naegle KM, et al. Injury-induced HDAC5 nuclear export is essential for axon regeneration. *Cell* 2013; 155: 894–908.
37. Wheeler DG, Barrett CF, Groth RD, et al. CaMKII locally encodes L-type channel activity to signal to nuclear CREB in excitation–transcription coupling. *J Cell Biol* 2008; 183: 849–863.
38. Rigo FK, Dalmolin GD, Trevisan G, et al. Effect of omega-conotoxin MVIIA and Phalphanalbeta on paclitaxel-induced acute and chronic pain. *Pharmacol Biochem Behav* 2013; 114–115: 16–22.
39. Roelofs RI, Hrushesky W, Rogin J, et al. Peripheral sensory neuropathy and cisplatin chemotherapy. *Neurology* 1984; 34: 934–938.
40. Xu L, Wang W, Chong J, et al. RNA polymerase II transcriptional fidelity control and its functional interplay with DNA modifications. *Crit Rev Biochem Mol Biol* 2015; 50: 503–519.
41. Chaney SG, Campbell SL, Bassett E, et al. Recognition and processing of cisplatin- and oxaliplatin-DNA adducts. *Crit Rev Oncol Hematol* 2005; 53: 3–11.
42. Jung Y and Lippard SJ. RNA polymerase II blockage by cisplatin-damaged DNA. Stability and polyubiquitylation of stalled polymerase. *J Biol Chem* 2006; 281: 1361–1370.
43. Yoon MS, Katsarava Z, Obermann M, et al. Erythropoietin overrides the triggering effect of DNA platination products in a mouse model of cisplatin-induced neuropathy. *BMC Neurosci* 2009; 10: 77.
44. Kelley MR, Jiang Y, Guo C, et al. Role of the DNA base excision repair protein, APE1 in cisplatin, oxaliplatin, or carboplatin induced sensory neuropathy. *PLoS One* 2014; 9: e106485.
45. Screnci D and McKeage MJ. Platinum neurotoxicity: clinical profiles, experimental models and neuroprotective approaches. *J Inorg Biochem* 1999; 77: 105–110.
46. Pannese E. The satellite cells of the sensory ganglia. *Adv Anat Embryol Cell Biol* 1981; 65: 1–111.
47. Pannese E. The structure of the perineuronal sheath of satellite glial cells (SGCs) in sensory ganglia. *Neuron Glia Biol* 2010; 6: 3–10.
48. Huang LY, Gu Y and Chen Y. Communication between neuronal somata and satellite glial cells in sensory ganglia. *Glia* 2013; 61: 1571–1581.
49. Joseph EK and Levine JD. Comparison of oxaliplatin- and cisplatin-induced painful peripheral neuropathy in the rat. *J Pain* 2009; 10: 534–541.
50. Ta LE, Bieber AJ, Carlton SM, et al. Transient Receptor Potential Vanilloid 1 is essential for cisplatin-induced heat hyperalgesia in mice. *Mol Pain* 2010; 6: 15.
51. Arama E, Agapite J and Steller H. Caspase activity and a specific cytochrome C are required for sperm differentiation in *Drosophila*. *Dev Cell* 2003; 4: 687–697.
52. Simon DJ, Weimer RM, McLaughlin T, et al. A caspase cascade regulating developmental axon degeneration. *J Neurosci* 2012; 32: 17540–17553.
53. Ip V, Liu JJ, Mercer JF, et al. Differential expression of ATP7A, ATP7B and CTR1 in adult rat dorsal root ganglion tissue. *Mol Pain* 2010; 6: 53.